Sensors **2006**, *6*, 1411-1419

sensors

ISSN 1424-8220

http://www.mdpi.org/sensors

Review

Photoacoustic Spectroscopy with Quantum Cascade Lasers for Trace Gas Detection

Angela Elia *, Cinzia Di Franco, Pietro Mario Lugarà and Gaetano Scamarcio

LIT^3 CNR-INFM Regional Laboratory, Department of Physics - University of Bari, Via Amendola 173, I-70126 Bari, Italy

E-mail: angela.elia@fisica.uniba.it (A. Elia). E-mail: cinzia.difranco@fisica.uniba.it (C. Di Franco). E-mail: lugara@fisica.uniba.it (P.M. Lugarà). E-mail: scamarcio@fisica.uniba.it (G. Scamarcio)

* Author to whom correspondence should be addressed.

Received: 4 October 2006 / Accepted: 25 October 2006 / Published: 27 October 2006

Abstract: Various applications, such as pollution monitoring, toxic-gas detection, non invasive medical diagnostics and industrial process control, require sensitive and selective detection of gas traces with concentrations in the parts in 10^9 (ppb) and sub-ppb range.
The recent development of quantum-cascade lasers (QCLs) has given a new aspect to infrared laser-based trace gas sensors. In particular, single mode distributed feedback QCLs are attractive spectroscopic sources because of their excellent properties in terms of narrow linewidth, average power and room temperature operation. In combination with these laser sources, photoacoustic spectroscopy offers the advantage of high sensitivity and selectivity, compact sensor platform, fast time-response and user friendly operation. This paper reports recent developments on quantum cascade laser-based photoacoustic spectroscopy for trace gas detection. In particular, different applications of a photoacoustic trace gas sensor employing a longitudinal resonant cell with a detection limit on the order of hundred ppb of ozone and ammonia are discussed. We also report two QC laser-based photoacoustic sensors for the detection of nitric oxide, for environmental pollution monitoring and medical diagnostics, and hexamethyldisilazane, for applications in semiconductor manufacturing process.

Keywords: photoacoustic spectroscopy, quantum cascade laser, trace gas detection.

---

1. Introduction

The detection and quantification of trace gases is of great interest in a wide range of applications such as pollution monitoring, industrial process control, toxic-gas detection and human breath analysis for medical diagnostics. These applications require trace gas sensors characterized by high sensitivity (ppb or sub-ppb levels) and selectivity (to avoid interferences from other potential interfering species), multi-component capability, real time and continuous measurements, large dynamic range, in situ measurements, ease and autonomous of operation.

Today, there are different spectroscopic methods which can potentially meet many of these requirements. In addition, the recent development of quantum cascade lasers offers interesting light sources for laser-based gas sensors operating in the mid-infrared spectral region where the molecular absorptions are stronger than in the near-infrared [1].

In particular, photoacoustic spectroscopy (PAS) represents a very attractive technique for sensitive trace gas detection. PAS is based on the generation of an acoustic wave in a gas cell resulting from the absorption of modulated light of appropriate wavelength by molecules. The amplitude of this sound wave is directly proportional to the gas concentration and can be detected using a sensitive microphone if the laser beam is modulated in the audio frequency range.

In combination with quantum cascade lasers (QCLs), PAS offers the advantage of high sensitivity (ppb detection limits), large dynamic range (linearity over a range of 10^6) compact set-up, fast time-response and simple optical alignment, if compared with other competing detection schemes, such as multi-pass absorption spectroscopy [2,3] or cavity ringdown spectroscopy [4], which offer similar performances, but require more sophisticated equipments.

In this review we report recent developments on quantum cascade laser-based photoacoustic spectroscopy for trace gas detection. After a preliminary section describing the fundamentals of photoacoustic spectroscopy, the paper is divided into two sections. In the first one, we present some trace gas detection schemes based on QCLs which prove the potentialities of these new light sources. In the second section, we report a number of selected applications of photoacoustic spectroscopy with QCLs demonstrated worldwide by several groups [5-9].

2. Photoacoustic spectroscopy

2.1. Theoretical background

The generation and the detection of the PA signal can be divided into three main steps [10,11]:

(1) Absorption of modulated light of appropriate wavelength by molecules and heat release in the gas sample due to non-radiative relaxation (molecular collisions) of the excited states.

(2) Generation of an acoustic wave due to the periodic heating of the gas sample.

(3) Detection of the acoustic signal in the photoacoustic cell.

In the case of small absorption ($\alpha << 1$) and intensities (no saturation of molecular transition) and for modulation frequencies that fulfil the condition $\omega\tau << 1$ (ω in the kilohertz range or below, τ is the total lifetime of the excited states), the heat production rate $H(r,t)$ is directly proportional to the molecular absorption coefficient α and to the radiation intensity $I(r,t) = I_0(r)e^{i\omega t}$. Its modulation directly follows the modulation of the incident radiation:

$$H(r,t) = \alpha I_0(r)\, e^{i\omega t} \tag{1}$$

The inhomogeneous wave equation relating the acoustic pressure p and the heat source H is

$$\frac{\partial^2 p}{\partial t^2} - c^2 \nabla^2 p = (\gamma - 1)\frac{\partial H}{\partial t} \tag{2}$$

here c indicates the sound speed in the gas and $\gamma = C_p / C_V$ the ratio of specific heats. In this equation the dissipative terms due to viscosity and thermal conduction are neglected.

For a sinusoidal modulation of the incident radiation with an angular frequency ω, the Fourier transform of the pressure amplitude p is expressed as a superposition of normal acoustic modes:

$$p = p(r,\omega) = \sum_j A_j(\omega)\, p_j(r) \tag{3}$$

where A_j is the complex amplitude of the normal mode j and p_j are the solutions of the homogeneous wave equation:

$$\left(\nabla^2 + \frac{{\omega_j}^2}{c^2}\right) p_j(r) = 0 \tag{4}$$

which satisfy the boundary condition of vanishing normal gradient at the cell walls.

The PA signal measured by a pressure sensor, usually a microphone, is given by

$$S = C \cdot P(\lambda) \cdot \alpha(\lambda) \tag{5}$$

where C is the cell constant in the unit of Vcm/W, P the optical power of the laser source and α the absorption coefficient which is related to the gas concentration (N, number density of molecules) and absorption cross section (σ) by $\alpha = N\sigma$.

2.2. Cylindrical photoacoustic cell

The orthonormal modes for cylindrical geometry of the PA cell are given by the superposition of longitudinal, azimuthal and radial modes identified by the eigenvalues l, m and n respectively [11]. The corresponding angular frequency is given by:

$$\omega_j = 2\pi f_j = \pi c \left[\left(\frac{l}{L}\right)^2 + \left(\frac{\alpha_{mn}}{R}\right)^2 + \left(\frac{n}{R}\right)^2\right]^{1/2} \tag{6}$$

where R and L respectively indicate the radius and the length of the cylindrical cell and α_{mn} is the zero of order n of the equation $\partial J_m / \partial r = 0$ with J_m the Bessel function of order m.

The Fourier coefficient $A_j(\omega)$ is given by:

$$A_j(\omega) = -\frac{i\omega(\gamma - 1)}{\left({\omega_j}^2 - \omega^2 - i\omega\omega_j / Q_j\right) V_o} \frac{1}{V_o} \int_{V_o} p_j^* H dV \tag{7}$$

which takes the orthonormal conditions for the eigenfunctions p_j and the mode damping into account and where V_o is the cell volume, Q the quality factor of the resonance and the integral describes the geometrical coupling between laser radiation and the acoustical mode.

If the modulation frequency is equal to one of the acoustical eigenfrequencies of the cavity ($\omega = \omega_j$), the energy is accumulated in a standing wave and its amplitude is amplified in comparison to a non resonant cell ($\omega_j = 0$) by a factor equal to the quality factor Q.

3. Quantum cascade lasers for trace gas detection

The recent development of quantum-cascade lasers offers an attractive new option for the development of laser-based gas sensors and high resolution spectroscopic applications [1]. Based on intersubband transition in a multiple-quantum-well heterostructure, the emission wavelength of QCLs can be tailored over a wide spectral range in the mid-infrared, using band-structure engineering. In particular, single mode quantum cascade lasers have become very attractive for mid-infrared gas sensing techniques thanks to tunability in the spectroscopically important region from 3 to 20 μm (fingerprint region), where many polluting gases exhibit strong fundamental ro-vibrational absorption transitions which are one or two orders of magnitude more intense than overtone or combination band in the near infrared. Moreover, single mode distributed feedback (DFB) quantum cascade lasers show excellent properties in terms of narrow linewidth, average power (tens of milliwatt) and room temperature operation and their implementation has the potential of considerably improved flexibility. They overcome some of the major drawbacks of other traditional mid-IR laser sources: lack of continuous wavelength tunability and large size and weight of gas lasers (e.g. CO and CO_2), low output power and cooling requirement of lead salt diode lasers, complexity and low power of nonlinear optical sources.

Since 1998, when DFB-QCL were demonstrated for the first time in trace gas sensing applications [12], several trace gas detection schemes based on DFB-QCL have been developed and the number of applications is rapidly increasing in particular in medicine and pollution monitoring.

Kosterev et al. [4] reported a spectroscopic gas sensor for nitric oxide (NO) detection based on the cavity ringdown technique. A continuous wave (CW) QC-DFB laser operating at 5.2 μm was used as a tunable single-frequency light source. Measurements of parts per billion (ppb) NO concentrations in pure N_2 with a sensitivity of 0.7 ppb for a data collection time of 8 s were performed.

Weidmann et al. [13] reported the development of a gas sensor based on long-path absorption and a quantum cascade laser for the detection of ethylene (C_2H_4). The laser, operated in a pulsed mode at a wavelength of ~10 μm, was thermoelectrically cooled. Gas absorption was recorded in a 100-m optical pathlength astigmatic Herriott cell. With a 10-kHz pulse repetition rate and an 80-s total acquisition time, a noise equivalent sensitivity of 30 parts per billion was demonstrated. The sensor was applied to monitor C_2H_4 in vehicle exhaust as well as in air collected in a high-traffic urban tunnel.

Menzel et al. [2] monitored NO in exhaled human breath using quantum cascade laser-based cavity-enhanced spectroscopy (CES) with an effective path length of 670 m. The distributed feedback QCL operated in continuous wave at liquid nitrogen temperature near $\lambda = 5.2$ μm. The minimum detectable NO concentration was found to be 16 ppb. The same group has recently reported [14] off-axis CES, combined with a wavelength-modulation technique, with a thermoelectrically cooled, cw DFB QCL operating at 5.45 μm for the detection of NO with sub-ppb detection limits. They used a 50-cm-long high-finesse optical cavity with an effective path length of 700 m. A noise equivalent minimum detection limit of 0.7 ppb with a 1-s observation time was achieved.

4. Photoacoustic spectroscopy with quantum cascade laser

In recent years quantum cascade lasers have also been successfully used in combination with photoacoustic spectroscopy for the detection of gas traces with concentrations in the ppb range. The

most important applications and results are summarized in table 1.

Table 1. Summary of selected published results on QCL-based photoacoustic spectroscopy gas sensing.

Reference	**[7]**	**[6]**	**[5]**	**[8]**	**[9]**
Chemicals	H_2O, NH_3	NH_3, CO_2, CH_3OH	O_3	NO	HMDS
Laser source	8.5 μm DFB QCL, CW, P= 16 mW	10.2 μm DFB QCL, pulsed, duty cycle 3-4% P= 2 mW	9.5 μm DFB QCL, pulsed, duty cycle 2% P= 2-4.6 mW	5.3 μm DFB QCL, pulsed, duty cycle 1.4% P< 8 mW	8.4 μm Fabbry Perrot QCL, pulsed, duty cycle 0.0014% P< 1 mW
PA Cell	First longitudinal mode, 1.66 KHz	Multipass cell, First longitudinal mode, 1.25 KHz, 16 microphones	Differential cell, First longitudinal mode, 3.8 KHz,	First longitudinal mode, 1.38 KHz, 4 microphones	First longitudinal mode, 1.38 KHz, 4 microphones
Detection limit	100 ppb for NH_3 (10 min.)	300 ppb for NH3 at 400 mbar, $\alpha_{min}=2.2\times10^{-5}$ cm^{-1}	102 ppb, $\alpha_{min}=1.24\times10^{-6}$ cm^{-1}	500 ppb, $\alpha_{min}=4.4\times10^{-6}$ cm^{-1}	200 ppb,

4.1. Review of selected published results

Paldus et al. [7] reported photoacoustic spectra of ammonia (NH_3) and water vapor (H_2O) using a CW cryogenically cooled QC-DFB laser emitting at 8.5 μm with a 16 mW power output. They used a PAS resonant cell (1.66 kHz) which consisted of an acoustic resonator (100 mm long, gold-coated copper) and two buffer volumes (50 mm long) introduced to reduce the background signal due to the heating of the two ZnSe Brewster windows. The laser beam intensity was modulated at 1.66 KHz using a mechanical chopper. The QC-DFB was scanned in wavelength over 35 nm by temperature tuning for generation of absorption spectra or temperature stabilized for real-time concentration measurements. Photoacoustic measurements were obtained for concentrations ranging from 2200 ppmv to 100 ppbv. The detection limit of ammonia was 100 ppbv at standard temperature and pressure with a measurement time of 10 minutes.

Hofstetter et al. [6] reported PAS measurement of carbon dioxide (CO_2), methanol (CH_3OH) and ammonia using a pulsed 10.4 μm QC-DFB laser operated at 3-4% duty cycle with 25 ns long current pulses (2 mW average power) and close to room temperature. The QC-DFB was scanned in wavelength over 3 cm^{-1} by temperature tuning with a linewidth of 0.2 cm^{-1}. They used a resonant multi-pass PAS cell consisting of an acoustic resonator (120 mm long, gold-coated copper) and two

buffer volumes (60 mm long) integrated into a Herriott multipass arrangement (36 passes with an effective pathlength of 15 m). The PAS cell was equipped with a radial 16-microphone array to increase sensitivity. The laser beam intensity was mechanically chopped at the first longitudinal resonance (Q=70) of the PAS cell (1.25 kHz). The ammonia detection limit was 300 ppb, which corresponds to a minimum measurable absorption coefficient of $\alpha_{min}=2.2\times10^{-5}$ cm^{-1}, with a signal-to-noise ratio (SNR) of 3 and a pressure of 400 mbar. PA absorption spectra of CO_2, CH_3OH and NH_3 were also reported.

More recently, *Da Silva et al.* [5] have reported the PAS measurement of ozone (O_3) with a commercial DFB-QCL (Alpes Lasers) emitting at 9.5 μm and working in pulsed operation (duty cycle 2 % and 50 ns long current pulses for determination of concentrations, duty cycle 0.8 % and 20 ns long current pulses for determination of spectra) near room temperature (thermoelectrically cooled). The QCL (2 – 4.6 mW average power) was modulated by an external TTL signal at 3.8 KHz to excite the first longitudinal mode of the differential PAS cell (with a Q=36). PA spectra were measured by scanning the wavelength of the QCL by temperature tuning. Photoacoustic measurements were performed for concentrations ranging from 4300 ppmv to 100 ppbv. The detection sensitivity of ~100 ppbV corresponds to a minimum measurable absorption coefficient of $\alpha_{min}=1.24\times10^{-6}$ cm^{-1} with a SNR of 1.

4.2. Photoacoustic detection of nitric oxide and hexamethyldisilazane

In our laboratories we have developed quantum cascade laser-based photoacustic sensors interesting for trace gas detection in pollution monitoring, industrial process control and medical diagnostic with a detection limit on the order of hundred parts in 10^9. The photoacoustic spectrometer consists of an amplitude modulated QCL, a photoacoustic cell and a signal acquisition and processing equipment. A schematic diagram of the spectrometer is shown in Fig. 1. The resonant PAS cell is a cylindrical stainless steel resonator of 120 mm length and 4 mm radius with λ/4 buffer volumes on each side used as acoustic filters. The cell is closed by two antireflection (AR) coated ZnSe windows. The resonator operates in the first longitudinal mode at 1380 Hz and is equipped with 4 electret microphones (Knowles EK 3024, 20 mV/Pa, 0.5 μV/Hz-1), placed at the position of maximum acoustic amplitude to increase the signal-to-noise ratio. The electrical signals of the microphones are preamplified and then measured by a digital lock-in amplifier (EG&G Instruments) with a 10 s integration time constant.

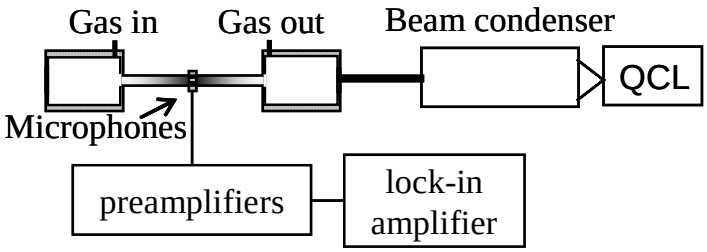

Figure 1. Block diagram of the PAS spectrometer.

We have developed a PAS trace gas sensor for the measurement of nitric oxide [8]. The detection of NO in the ppb range plays an important role in monitoring the environmental pollution and in medical

diagnostics. NO is formed during high temperature combustion processes, such as car exhaust, it is implicated in the depletion of the ozone layer, the generation of photochemical smog and acid rains [15]. More recently it has been demonstrated that NO is involved in several biological functions and human pathologies; it has been proved that NO detection in human breath is effective in non-invasive diagnostic technique for monitoring of asthma and inflammatory lung diseases [16, 17].

Various effective spectroscopic methods have been reported for NO detection in ppb and sub-ppb range, such as cavity ringdown spectroscopy [4], multipass absorption spectroscopy, cavity-enhanced spectroscopy (CES) [2] and tunable infrared laser differential absorption spectroscopy (TILDAS) [3].

The photoacoustic trace gas sensor for the measurement of NO is based on a commercially available distributed feedback quantum cascade laser (Alpes Laser) operated in pulsed mode (pulse duration of 42 ns and a duty cycle of 1.4%) with an optical average power of 8 mW at a wavelength around 5.3 μm. Its light was collected with an AR coated ZnSe lens and collimated by a beam condenser (0.2X). The laser beam intensity was modulated by a mechanical chopper at the first longitudinal resonance frequency of the photoacoustic cell. The PAS signal for different nitric oxide concentration was measured by tuning the laser emission over the P(1.5) NO lines. These lines, located at 1871.051-1871.066 cm^{-1}, have a maximum intensity of 0.8×10^{-20} cm/molecule and are well separated from the nearest interfering H_2O and CO_2 absorption lines. The PAS signal was measured in the 495 ppmv - 500 ppbv concentration range. The detection limit for NO measurement is 500 ppb and the sensitivity of the apparatus is essentially limited by the background noise level. The minimum detectable absorption coefficient at SNR=1 is $\alpha_{min}=4.4\times10^{-6}$ cm^{-1}, and the minimum detectable absorption coefficient normalized to power and detection bandwidth is 1.1×10^{-7} $cm^{-1}W/Hz^{1/2}$.

We have also studied the feasibility of using QCL-PAS sensors for the detection of toxic gases in the semiconductor industry. We focused on the trace detection of HMDS and obtained a minimum detection limit of 200 ppb [9]. HMDS is a compound widely used in photolithography as photoresist adhesion promoter to the semiconductor substrate. Its high volatility and low water solubility make HMDS potentially risky for the health. We used a non-commercial Fabry-Perot ridge waveguide QCL with a superlattice active region and a relaxation-stabilized injector [18], emitting a peak power of 2 W at temperatures below 120 K and several 100 mW at room temperature. The multimode laser emission is located around 1185 cm^{-1} where the HMDS absorption spectrum is characterized by the intense N–H bending mode band (1183 cm^{-1}, full width at half maximum ~ 15 cm^{-1}) with an integrated band strength of 7×10^{-19} cm/molecule. The laser was mounted in a helium closed-cycle cryostat, working at 20 K. The optical power was modulated at the acoustic frequency of the cell using a pulse generator. The radiation was collected by an AR coated ZnSe lens and collimated by a beam condenser to a parallel beam of 5 mm diameter, in order to prevent the interaction of QCL radiation with the cell walls. All the photoacoustic measurements were performed at a duty cycle of 0.014% (100 ns pulse length). To calibrate the system and determine the detection limit it was necessary to prepare a gas sample with known HMDS dilution (142 parts in 10^6) by using a full evaporation technique [19]. Subsequent dilutions with purified N_2 allowed to obtain even lower concentrations. A minimum detectable concentration of 200 ppb was obtained, essentially limited by the background signal (~500 μV) measured by filling the PAS cell with pure nitrogen. It was due to the periodical heating of the PAS cell windows and walls and to desorb residual gas traces. The contribution of external acoustic

and electromagnetic noises, mainly uncorrelated with the modulation frequency, was detected with the QCL beam blocked.

The reduction of external acoustic and electrical noises may further increase the signal-to-noise-ratio and thereby reduce the detection limit.

Conclusions

In this paper we have reviewed the state of art of quantum cascade laser-based photoacoustic spectroscopy for trace gas detection. Different applications demonstrate the effectiveness of this technique for sensitive, selective, real time trace gas concentration measurements. In fact, the sensitivity limits demonstrated are surely interesting for several applications in ppb range. In addition to this, the forthcoming commercial availability of recently demonstrated single-mode QCLs operating in continuous wave at room temperature [20-22] will result in a significant improvement of the sensitivity up to sub-ppb detection limits. Moreover, PA detectors are considerably simpler and cheaper than other competing detection schemes which offer similar performances, but require more sophisticated equipments.

Acknowledgements

The authors gratefully acknowledge partial financial support by INFM under MIUR contracts FIRB “MIAO” (RBNE01-BSXF) and DD1105/2002.

References

1. Kosterev, A.A.; Tittel, F. Chemical sensors based on quantum cascade lasers. *IEEE J. Quantum Electron.* **2002**, *38(6)*, 582–591.
2. Menzel, L.; Kosterev, A.A.; Curl, R.F.; Tittel, F.K.; Gmachl, C.; Capasso, F.; Sivco, D.L.; Baillargeon, J.N.; Hutchinson, A.L.; Cho, A.Y.; Urban, W. Spectroscopic detection of biological NO with a quantum cascade laser. *Appl. Phys B* **2001**, *72*, 859-863.
3. Nelson, D.D.; Shorter, J.H.; McManus, J.B.; Zahniser, M.S. Sub-part-per-billion detection of nitric oxide in air using a thermoelectrically cooled mid-infrared quantum cascade laser spectrometer. *Appl. Phys. B* **2002**, *75*, 343-350.
4. Kosterev, A.A.; Malinovsky, A.L.; Tittel, F.K.; Gmachl, C.; Capasso, F.; Sivco, D.L.; Baillargeon, J.N.; Hutchinson, A.L.; Cho, A.Y. Cavity ringdown spectroscopic detection of nitric oxide with a continuous-wave quantum-cascade laser. *Appl. Opt.* **2001**, *40*, 5522-5529.
5. Da Silva, M.G.; Vargas, H.; Miklós, A.; Hess, P. Photoacoustic detection of ozone using a quantum cascade laser. *Appl. Phys. B* **2004**, *78*, 677-680.
6. Hofstetter, D.; Beck, M.; Faist, J.; Nagele, M.; Sigrist, M.W. Photoacoustic spectroscopy with quantum cascade distributed-feedback lasers. *Opt. Lett.* **2001**, *26*, 887-889.
7. Paldus, B.A.; Spence, T.G.; Zare, R.N.; Oomens, J.; Harren, F.J.M.; Parker, D.H.; Gmachl, C.; Capasso, F.; Sivco, D.L.; Baillargeon, J.N.; Hutchinson, A.L.; Cho, A.Y. Photoacoustic spectroscopy using quantum cascade lasers. *Opt. Lett.* **1999**, *24*, 178-180.

8. Elia, A.; Lugarà, P.M.; Giancaspro C. Photoacoustic detection of nitric oxide by use of a quantum cascade laser. *Opt. Lett.* **2005**, *30(9)*, 988-990.
9. Elia, A.; Rizzi, F.; Di Franco, C.; Lugarà, P.M.; Scamarcio, G. Quantum cascade laser-based photoacoustic spectroscopy of volatile chemicals: application to hexamethyldisilazane. *Spectrochimica Acta A* **2006**, *64*, 426-429.
10. Kreuzer, L.B. in *Optoacoustic spectroscopy and detection*; Pao,Y.-H., Ed; Accademic Press: New York, 1977, 1-25.
11. Sigrist, M.W. in *Air Monitoring by Spectroscopic techniques*; Sigrist, M.W., Ed.; Wiley: New York, 1994, 163–227.
12. Sharpe, S.W.; Kelly, J.F.; Hartman, J.S.; Gmachl, C.; Capasso, F.; Sivco, D.L.; Baillargeon, J.N.; Cho, A.Y. High-resolution (Doppler-limited) spectroscopy using quantum-cascade distributed-feedback lasers. *Opt. Lett.* **1998**, *23*, 1396–1398.
13. Weidmann, D.; Kosterev, A.A.; Roller, C.; Curl, R.F.; Fraser, M.P.; Tittel, F.K. Monitoring of ethylene by a pulsed quantum cascade laser". *Appl. Opt.* **2004**, *43(16)*, 3329-3334.
14. Bakhirkin, Y.A.; Kosterev, A.A.; Curl, R.; Tittel, F.K.; Yarekha, D.A.; Hvozdara, L.; Giovannini, M.; Faist, J. Sub-ppbv nitric oxide concentration measurements using cw thermoelectrically cooled quantum cascade laser-based integrated cavity output spectroscopy. *Appl. Phys. B* **2006,** *82*, 149-154.
15. Seinfeld J.H., Pandis S.N. *Atmospheric Chemistry and Physics: From Air Pollution to Climate Change*; John Wiley & Sons: New York, 1998.
16. Alving, K.; Weitzberg, E.; Lundberg, J.M. Increased amount of nitric oxide in exhaled air of asthmatics. *Eur. Respir. J.* **1993**, *6*, 1368- 1370.
17. Wilson N.; Pedersen, S. Inflammatory markers in clinical practice. *Am. J. Respir. Crit. Care Med.* **2000**, *162*, 485-515.
18. Scamarcio, G.; Troccoli, M.; Capasso, F.; Hutchinson, A.L.; Sivco, D.L.; Cho. A.Y. High peak power (2.2 W) superlattice quantum cascade laser. *Electronics Lett.* **2001**, *37(5)*, 1-2.
19. Markelov**,** M.; Guzowski, J.P. Matrix independent headspace gas chromatographic analysis. The full evaporation technique. *Anal. Chim. Acta* **1993**, *276*, 235-245.
20. Beck, M.; Hofstetter, D.; Aellen, T.; Faist, J.; Oesterle, U.; Ilegems, M.; Gini, E.; Melchior, H. Continuous wave operation of a mid-infrared semiconductor laser at room temperature. *Science* **2002**, *295*, 301-305.
21. Yu, J.S.; Slivken, S.; Darvish, S.R.; Evans, A.; Gokden, B.; Razeghi, M. High-power, room temperature and continuous-wave operation of distributed-feedback quantum-cascade lasers at λ=4.8 mm. *Appl. Phys. Lett*. **2005**, *87(4)*, 041104.
22. Darvish, S.R.; Slivken, S.; Evans, A.; Yu, J.S.; Razeghi, M. Room-temperature, high-power, and continuous-wave operation of distributed-feedback quantum-cascade lasers at λ~9.6 μm**.** *Appl. Phys. Lett.* **2006,** *88*, 201114.
23. Diehl, L.; Bour, D.; Corzine, S.; Zhu, J.; Höfler, G.; Lončar, M. ; Troccoli, M.; Capasso, F. High-power quantum cascade lasers grown by low-pressure metal organic vapor-phase epitaxy operating in continuous wave above 400 K. *Appl. Phys. Lett.* **2006,** *88*, 201115.